

## Numerical simulation of three phase asynchronous motor to diagnose precisely the stator unbalanced voltage anomaly

### Simulation numérique du moteur asynchrone triphasé pour diagnostiquer précisément le défaut du déséquilibre de tension d'alimentation

Nadir Benamira<sup>1\*</sup>, Mohamed Faouzi Rachedi<sup>2</sup>, Slimane Bouras<sup>3</sup>,

Samir Kerfali<sup>4</sup> & Ahmed Bouraiou<sup>5</sup>

<sup>1,2</sup> Electromechanical systems laboratory, department of electromechanical engineering, Badji Mokhtar-Annaba University, P.O. Box 12, 23000, Annaba, Algeria.

<sup>3,4</sup> Electromechanical engineering laboratory, Badji Mokhtar-Annaba University, P.O. Box 12, Annaba, 23000, Algeria.

<sup>5</sup> Research unit in renewable energies in the saharan medium, URER-MS, P.O.Box 478, 01000 Adrar, Algeria.

Soumis le 02/09/2015

Révisé le 26/09/2016

Accepté le 17/10/2016

#### ملخص

سلسلة من عمليات المحاكاة الرقمية لاختلال توازن التوتر تم القيام بها على محرك لا متزامن من أجل دراسته الحالات الغير طبيعية للمحرك. أولاً تم استعمال التمثيل البياني للتيارات الكهربائية لتشخيص أولي من جهة، ومن جهة أخرى قمنا أيضاً باستعمال طريقة شعاع بارك الموسعة (EPVA). وعليه تم الحصول على شكل إهليلجي وعنصر توافقي ثاني لهاتين الطريقتين على التوالي. إن هذه الآثار غالباً ما تعتبر في أبحاث أخرى كمؤشرات مباشرة ودقيقة على خلل الدارة الكهربائية القصيرة. هذا التماثل يؤدي إلى غموض عند الكشف عن العيوب مما يجعل القيام بتقنيات تكميلية إضافية أمر ضروري. إن التركيز على العنصر التوافقي الثاني (2.fs) المتعلق بطيف عزم الدوران (طريقة THA) قد بين فعاليته كمؤشر على اختلال التوازن. وعليه فإن (THA) هي وسيلة مثالية للتمييز بين العيوب.

**الكلمات المفتاحية :** المحركات الغير متزامنة، اختلال توازن التيار الكهربائي، تشخيص الأعطاب، التمثيل البياني للتيارات الكهربائية، طريقة شعاع بارك الموسعة، تحليل طيف عزم الدوران.

#### Résumé

Une série de tests de simulation du déséquilibre de tension d'alimentation, ont été effectués sur la machine asynchrone triphasée afin d'étudier les conditions anormales. Le modèle de données des courants statoriques est utilisée comme un diagnostic préliminaire. L'approche étendue du vecteur de Park (EPVA) est utilisé aussi. Un model elliptique et une 2ème composante harmonique sont obtenus par ces deux méthodes respectivement. Ces signatures dans d'autres recherches sont souvent considérées comme des indicateurs directs et précis du défaut de court-circuit du stator. Cette similitude mène à une incertitude dans la détection du défaut, ce qui rend l'utilisation de technique complémentaire impératif. La concentration sur la 2ème harmonique de la fréquence d'alimentation (2.fs) dans le spectre de couple (la méthode de THA) a montré son efficacité en tant que bon indicateur du déséquilibre de la tension. A cet effet, pour faire la distinction entre ces défauts, la THA est considéré comme l'outil idéal dans ce but.

**Mots clés :** motor à induction, déséquilibre de tension d'alimentation, diagnostic des défauts, modele des courants statorique, EPVA, THA.

#### Abstract

In the present paper, series of simulation tests of voltage unbalance, have been performed on triphase induction motor to study this unhealthy condition. First, the stator currents data pattern is used as a preliminary diagnosis. Secondly the extended Park's vector approach (EPVA) is also used. An elliptic pattern and a 2nd harmonic component are obtained by these two methods respectively. These signatures in other researches are often considered as direct and accurate indicators of a stator winding fault. This similarity leads to uncertainty in the detection of the fault, which makes imperative the use of complementary technique. The focus on the 2nd harmonic of the supply frequency (2.fs) in the torque spectrum (THA technique) has shown its effectiveness as good indicator of voltage unbalances. Therefore, to distinguish between these faults, the THA is considered as the ideal tool for this purpose.

**Key words:** induction motors, stator voltage unbalance, fault diagnostics, stator currents pattern, EPVA, THA

\*Corresponding author: nadir-benamira@live.fr

## 1. INTRODUCTION

The three-phase induction motors with squirrel cage are essential components in most of today's industrial production processes, because of their reliability, simplicity of construction and mechanical robustness. Thus, a special attention is given to their operation and their availability. Condition monitoring of induction motors is a vital factor in achieving efficient and profitable operation. So the greatest challenge in the area of condition monitoring is the diagnosis of a fault before it becomes critical [1,2,3].

The IEC standard and the European Commission's report show that the induction motors in the power range of 0.75 kW to 4 kW represent a particularly attractive opportunity for electricity savings [4]. Induction motors can be exposed to various phenomena; the most of these machines are directly connected to the power grid. Hence, it is very important to clarify the effect of voltage unbalance on the characteristics of induction motors [2].

The voltage unbalance effects on induction motors are stated as reduction on efficiency, mechanical oscillations and highly unbalanced currents on the stator. These high currents lead to a temperature rise, therefore, the insulation of the electrical conductors in the stator, are affected [3] and considered as the weakest part of the squirrel cage induction motors. This thermal stress leads to a reduction of induction motor life time [5,6].

Voltage unbalance generates negative sequence component in the voltage, the intensity of the magnetic field in the air gap is proportional to the amplitude of the positive and/or negative-sequence. The direction of rotation of the field corresponding to the negative sequence is opposed to the one corresponding to the positive sequence. That is why, in the case of unbalanced voltage, the resulting magnetic field becomes elliptic rather than circular [3,6].

This flux negative sequence produces several undesirable effects such as increased copper losses in the stator and in the rotor and power and torque pulsations. These pulsations are caused by a supplementary torque with a double frequency of the applied voltage. All these effects lead to a shorter lifetime of the machine, and healthy motors may be out of service [7].

Previous works concerning on-line monitoring of current Park's Vector approaches and 3D currents data pattern, have shown that these approaches can be used for abnormal conditions of induction motors. The ellipticity in both 3D currents data pattern and Park's Vector representation and the 2nd harmonic component obtained from the extended Park's vector approach (EPVA) are often considered as indicators of stator winding fault. Reported works [8, 9,10] are pertinent in this regard. On the other hand, researches [11,12] consider these signatures as a sign of an unbalanced voltage, so the main disadvantage of these techniques is that the stator voltage unbalances are interpreted as stator winding faults and vice versa. Therefore, from a physical point of view, the fault is not noticeable.

The present paper aims to study how these techniques are influenced by the unbalanced supply voltage and to present the similarity between the obtained signatures of the voltage unbalance and the stator winding fault signatures obtained in the literature. Hence, the Park's vector approach, the 3D currents data pattern and the extended Park's vector approach can be considered as tools used for a preliminary diagnosis (just to locate the origin of the fault). Therefore, the need of a complementary technique is necessary, in this regard, the torque harmonic analysis (THA) is proposed as a direct and effective technique for the diagnosis of the stator voltage imbalance.

This study is an extended work of a previous research [6] and aims to study the voltage unbalances faults in a better, through other unbalances cases and new diagnosis techniques.

## 2. THEORETICAL DEVELOPMENTS AND METHODS

### 2.1. Background informations of the voltage unbalances

The appearance of some symptoms in the induction motors such as the vibrations, the increased noise levels and the temperature rises in the stator is not necessarily an evidence of an internal fault, like bearing faults or stator short-circuit. Because other reasons may cause these problems, the stator unbalanced voltage is an external fault, which may cause these symptoms. So, faults that affect the motor are divided into two parts: internal and external faults [6]. External faults should not be underestimated because the most of the diagnosis investigate the internal faults. Figure1 summarizes the various external faults.

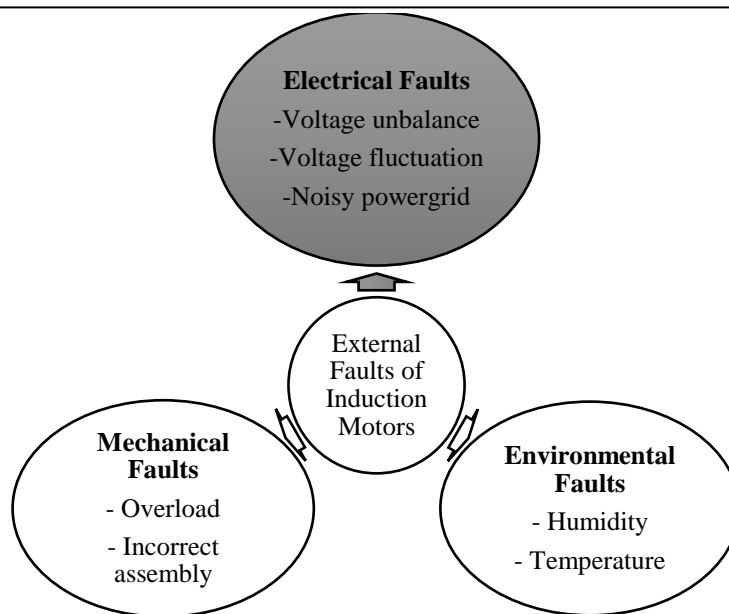


Figure.1. Classification of the external faults [6].

A three-phase system is unbalanced when the three-phase voltages and currents do not have the same amplitude and/or the same phase shift angle ( $120^\circ$ ). In order to analyze the performance of a three phase induction motor, symmetrical components analysis is normally used. In this method, positive and negative sequence equivalent circuits, as shown in Fig.2, are used to calculate different parameters of the machine under unbalanced voltage conditions [6].

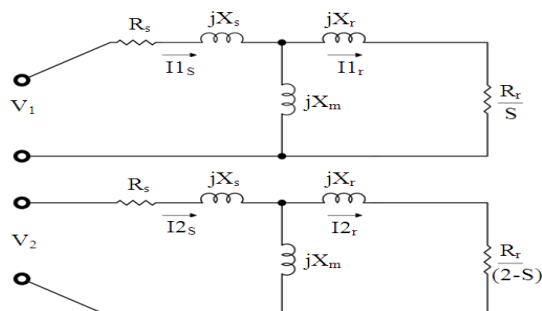


Figure. 2. Single-phase equivalent circuits of the motor: Positive-sequence (Top) and negative-sequence (Bottom)

In the equivalent circuit the subscripts  $s$  and  $r$  denote the stator and rotor, 1 and 2 refers the positive and the negative sequences respectively. Depending on the theories of symmetric components, all three-phase unbalanced systems can turn into two unbalanced three phase systems of different sequence plus a group of single phasors. The systems are positive, negative and zero sequences. So, with the complex values of voltages and currents of a three-phase system, the components of the sequence systems are [6]:

$$\begin{bmatrix} V_0 \\ V_1 \\ V_2 \end{bmatrix} = \frac{1}{3} \begin{bmatrix} 1 & 1 & 1 \\ 1 & a & a^2 \\ 1 & a^2 & a \end{bmatrix} \begin{bmatrix} V_A \\ V_B \\ V_C \end{bmatrix} \quad (1)$$

$$\begin{bmatrix} I_0 \\ I_1 \\ I_2 \end{bmatrix} = \frac{1}{3} \begin{bmatrix} 1 & 1 & 1 \\ 1 & a & a^2 \\ 1 & a^2 & a \end{bmatrix} \begin{bmatrix} I_A \\ I_B \\ I_C \end{bmatrix} \quad (2)$$

The subscripts A, B and C, refer to the three phase components of the real system, while 0, 1 and 2, are the zero, positive and negative sequence voltages and currents respectively; the operator ‘ $a$ ’ is:

$$a = 1 \angle 120^\circ$$

The International Electrotechnical Commission (IEC) introduces an independent definitions for voltage unbalance; it defines it as the ratio of the negative sequence voltage to the positive sequence voltage [5], this ratio, known as the voltage unbalance factor VUF, describes the voltage unbalance percentage [13]:

$$VUF = \left| \frac{V_2}{V_1} \right| 100\% \quad (3)$$

Figure 3 summarizes the eight different unbalanced voltage cases in any three phases systems [14].

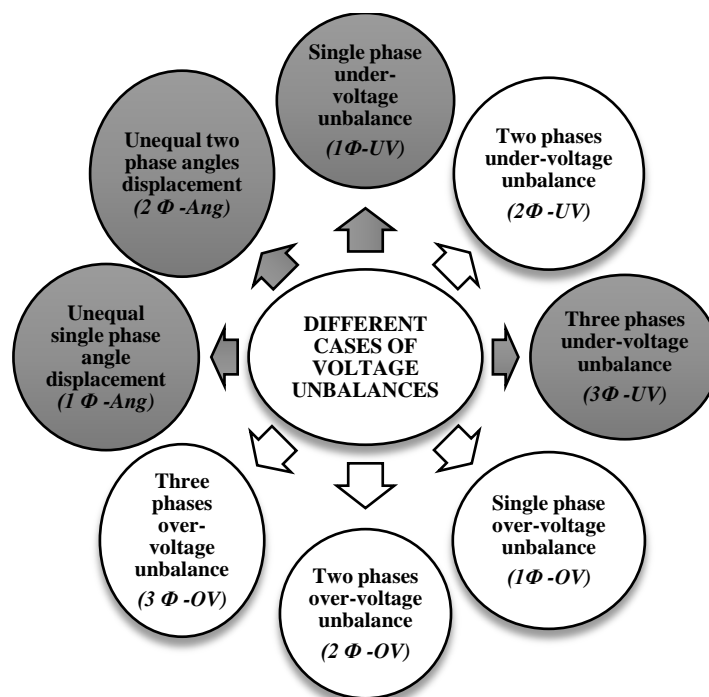


Figure. 3. The different unbalanced cases in the three phases systems

## 2.2. Theoretical principles of the analysis of balanced and unbalanced conditions

### 2.2.1. The stator currents data patterns

#### 2.2.1.1. Ideal operating condition

It's necessary to finish the investigation of the normal operating conditions, to develop a reference for comparison purposes. Most of the common methods used to identify faults in induction motor are based on the analysis of the stator currents. The Park's vector and the 3D current pattern approaches, also use the analysis of stator currents. However, in these methodologies, the fault detection will be converted into the pattern and depends on the change on it [15].

The obtained orbits have ellipsoidal, polygonal or hypocycloidal shapes according on the nature of the defect that occur on the drive [16]. Considering three-phase induction motors without neutral and ideal conditions and with unbalanced voltage supply, the stator currents are given by the following expressions [9,16]:

$$\begin{cases} I_A = I_m \sin(\omega t - \varphi) \\ I_B = I_m \sin(\omega t - \frac{2\pi}{3} - \varphi) \\ I_C = I_m \sin(\omega t - \frac{4\pi}{3} - \varphi) \end{cases} \quad (4)$$

Where:

$I_A, I_B$  and  $I_C$  = The three stator currents  
 $I_m$  = The maximum value of the supply phase current  
 $\omega$  = The supply frequency  
 $\varphi$  = The phase angle  
 $t$  = The time variable

The well-known Park transformation shows the variables of a three-phase machine through a system of two quadrature, they are a measuring and diagnostic tool in electric three-phase systems. The components of the stator current in a reference system formed by two orthogonal shafts which are fixed to the stator (shafts  $d$  and  $q$ ) are obtained by the following equation:

$$\begin{cases} i_d = \sqrt{\frac{2}{3}} I_A - \frac{1}{\sqrt{6}} I_B - \frac{1}{\sqrt{6}} I_C \\ i_q = \frac{1}{\sqrt{2}} I_B - \frac{1}{\sqrt{2}} I_C \end{cases} \quad (5)$$

where,  $i_d$  and  $i_q$  are the direct and quadrature axis currents respectively, under ideal operating conditions, when the supply currents constitute a positive sequence system, the three phase currents lead to a current Park's vector with the components:

$$\begin{cases} i_d = \frac{\sqrt{6}}{2} I_m \sin(\omega t) \\ i_q = \frac{\sqrt{6}}{2} I_m \sin(\omega t - \frac{\pi}{2}) \end{cases} \quad (6)$$

In Figure 4 (0% state of percentage of unbalance) the direct and quadrature currents axis represent a circle centered at the origin of the coordinators. These currents should ideally be  $\pi/2$  radians out of phase.

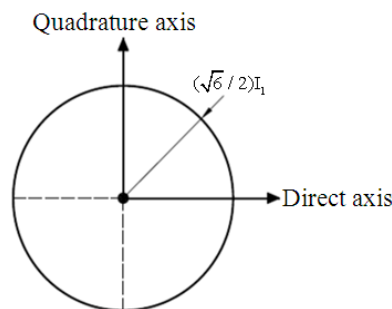


Figure.4. Current Park's vector representation for an ideal situation [8]

In the 3D stator current pattern, also we denote a circle centered at the origin of the coordinates, for ideal condition where its radius  $R$  is:

$$R^2 = I_A^2 + I_B^2 + I_C^2 \quad (7)$$

So, this circular pattern is an easy reference, that allows the detection and the identification of abnormal conditions by monitoring the deviations of acquired patterns [8].

In the case of a real healthy machine, the plot will differs slightly from a perfect circle for two main reasons first, practically all voltage sources contain some degree of asymmetry, i.e., the system is not perfectly balanced. Second, all electric machines contain some inherent asymmetries [11,17]. This result is considered as a baseline with respect to the case of abnormal condition.

### 2.2.1.2. Unbalanced operating condition

The stator asymmetry is a general concept of any stator unbalance, whether stator winding fault or/and voltage unbalance. So under these abnormal conditions, the equations (4) is no longer valid; the previous circle pattern no longer appears because the motor supply current will contain negative-sequence component besides the positive-sequence component. Fig.5 presents the induction motor currents under unbalanced condition.

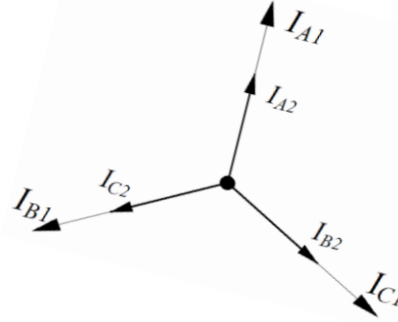


Figure.5. Induction motor currents under unbalanced voltage

$$\begin{cases} I_A = I_{A1} \sin(\omega t - \varphi) + I_{A2} \sin(\omega t - \varphi) \\ I_B = I_{B1} \sin\left(\omega t - \frac{2\pi}{3} - \varphi\right) + I_{C2} \sin\left(\omega t - \frac{4\pi}{3} - \varphi\right) \\ I_C = I_{C1} \sin\left(\omega t - \frac{4\pi}{3} - \varphi\right) + I_{B2} \sin\left(\omega t - \frac{2\pi}{3} - \varphi\right) \end{cases} \quad (8)$$

The motor supply current can be expressed as the sum of a positive and a negative- sequence components. Fig.6 presents the Park's vector plot with a stator asymmetry, its an elliptic pattern whose the amplitudes sum of the positive and negative-sequence components is directly proportional to the major axis, while the difference between the amplitudes of these two components is directly proportional to the length of the minor axis. The major axis orientation is associated with the faulty phase [6,8,10,12].

$$\begin{cases} i_d = \frac{\sqrt{6}}{2} (I_1 + I_2) \sin(\omega t) \\ i_q = \frac{\sqrt{6}}{2} (I_1 - I_2) \sin(\omega t - \frac{\pi}{2}) \end{cases} \quad (9)$$

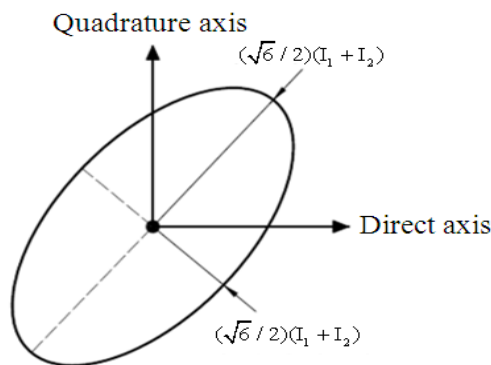


Figure. 6. Current Park's vector representation for a stator asymmetry [6,8]

As the stator currents differ from each other by 120° electrical, it is important to note that the three ellipses' major axis differ from each other by 120 spatial degrees in both park's vector approach and the 3-D current referential [9, 10].

Besides the recognition of the obtained elliptic pattern, the severity of the motor fault must be reported, which is related with the eccentricity of the ellipse. In this way, the new index is proposed, allowing the pattern identification and the fault severity measure. This severity index is given by equation (10), the parameters  $\lambda_{high}$  and  $\lambda_{low}$  denote respectively, the highest and lowest length of the ellipse axes. It is important to note that  $\lambda_{high}$  refers to the axis where the fault occurs-principal direction carrying more energy [9]. This severity index assumes values between zero and one, being the absence of any fault reported by a zero severity index ( $S_{st} = 0$ ) [9,10]:

$$S_{st} = 1 - \frac{\lambda_{low}}{\lambda_{high}} \quad (10)$$

### 2.2.2. The Enhanced Park's Vector Approach (EPVA)

In order to discriminate the information contained in the modulus of the current Park's vector, the EPVA is applied, which is the result of a spectral analysis of the Park's modulus temporal signal, the EPVA provides a more meaningful spectrum than the one obtained by the classical motor current spectral analysis [8].

$$i_M = \sqrt{(i_d(t))^2 + (i_q(t))^2} \quad (11)$$

where,  $i_M$  is the motor current Park's vector modulus.

#### 2.2.2.1. Ideal operating condition

In normal circumstances, the motor supply current contains only a positive sequence component, leading to a constant current Park's vector modulus. In these conditions, the EPVA signature will be clear from any spectral component. In the case of a real healthy machine the EPVA reveals the existence of a spectral component (100 Hz), with small amplitude, because there will be always a small degree of unbalance [8].

#### 2.2.2.2. Unbalanced operation condition

With an asymmetry in the stator the occurrence of the fault is manifested in the EPVA signature by the presence of a spectral component at a frequency of (100 Hz) twice the fundamental supply frequency [15]. Furthermore, the amplitude of this frequency is proportional to the severity of asymmetry. Figure 7 presents the Park's vector modulus with a stator unbalance.

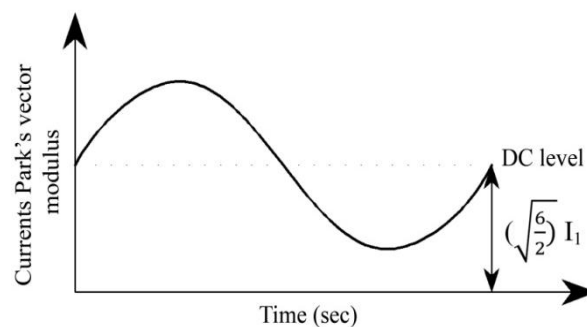


Figure 7. The motor current Park's vector modulus for a stator asymmetry [8]

### 2.2.3. Torque Harmonic Analysis (THA) for voltage unbalances detection

Temporal signal processing in the frequency domain is commonly encountered in diagnosis of induction motors. The THA and the stator Currents Spectral Analysis (MCSA) are powerful techniques for monitoring the health of induction motors, for the MCSA technique the two principal

spectral component that appear in case of voltage unbalance are the first and the third harmonics (50-150Hz) [12, 18]. Other researchers have turned to the use of the THA, in the case of unbalanced voltage, the component spectrum that appears is (100Hz) in the spectrum of the torque, this effective technique will be used in this research. The torque can be expressed by the following equation [6, 19, 20]:

$$T = \frac{P}{\omega} = \frac{P_0 + P_2}{\omega} = T_0 + T_2 \quad (12)$$

In order to simplify the survey, we suppose that the induction motor is an RL load, the torque will be written as follows:

$$T = \left( \frac{V.I}{\omega} \right) \cdot \eta \quad (13)$$

Where:

V = The input voltage

I = The current of each phase

$\eta$  = The motor efficiency

As we supposed previously, sinusoidal waveforms for voltage and current is applied, so the equation can be rewritten as:

$$T = K \cos(2\pi 50t + \alpha) \times \cos(2\pi 50t + \beta) \quad (14)$$

So:

$$T = K' \{ \cos(\alpha - \beta) + \cos(2\pi 100t + \alpha + \beta) \} \quad (15)$$

Based on this equation the resulting torque would include a DC term and a term with a fundamental frequency double of the frequency of applied voltage (2.fs). As expected, this component which is absent in normal operating condition, can detect and specify the relevance of the fault. So any kind of unbalance in the voltage in induction machines is detectable via torque harmonic analysis (THA).

### 2.3. Diagnostics algorithms

Figure 8 shows the flow charts of the stator asymmetry fault detection using all the techniques already cited and divided into two stages.

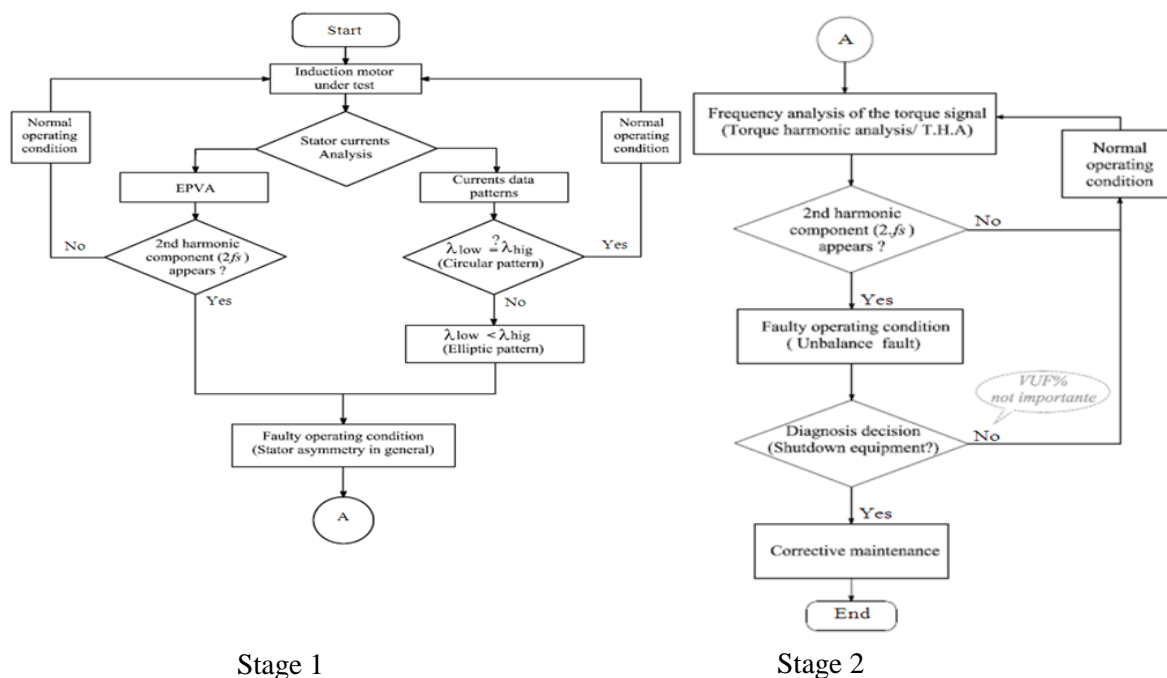


Figure.8. Flow charts of the proposed procedure of stator asymmetry diagnosis using currents data patterns, EPVA and THA approaches



### 3. SIMULATION TESTS

In this section, we present a great similarity between the unbalanced voltage and the stator winding fault, this similarity is a result of the emergence of the negative sequence in these two faulty cases. The mathematical model is simulated on MATLAB/Simulink, the unbalanced cases are created by imposing a modification in the voltage sources; the simulation is established under the following assumptions:

- 0.75 kW three phase induction motor, supplied by 311.12 (V) and 2.14 (A) peak for each phase;
- frequency  $f=50$  Hz ;
- No-load condition ;
- The repartition of the induction along the air gap is sinusoidal;
- Sinusoidal spatial distribution of magnetomotive forces air gap;
- Constant air gap, the effect of notches is negligible;
- No core losses .

Table 1 presents the different parameters of the unbalanced voltages cases studied, applied on the induction motor.

Table 1. Parameters of the balanced and unbalanced voltages circumstances studied

Balanced and unbalanced cases	Percentage of unbalance: amplitude or phase shift( $\theta^\circ$ )	$V_A \angle \text{Ang}^\circ$	$V_B \angle \text{Ang}^\circ$	$V_C \angle \text{Ang}^\circ$	Positive sequence voltage ( $V_1$ )	Negative sequence voltage ( $V_2$ )	Voltage unbalance factor VUF%	Type of pattern
Balanced	0% in all phases A,B and C	311.12 $\angle 0$	311.12 $\angle -120$	311.12 $\angle -240$	311.12	0.00	0.00	Circular
1 $\Phi$ -UV	10% in A	280 $\angle 0$	311.12 $\angle -120$	311.12 $\angle -240$	300.74	10.37	3.44	Elliptic
1 $\Phi$ -UV	20% in A	248.89 $\angle 0$	311.12 $\angle -120$	311.12 $\angle -240$	290.37	20.74	7.14	Elliptic
1 $\Phi$ -UV	20% in B	311.12 $\angle 0$	248.89 $\angle -120$	311.12 $\angle -240$	290.37	10.37	3.57	Elliptic
1 $\Phi$ -UV	20% in C	311.12 $\angle 0$	311.12 $\angle -120$	248.89 $\angle -240$	290.37	10.37	3.57	Elliptic
3 $\Phi$ -UV	10% in all phases	280 $\angle 0$	280 $\angle -120$	280 $\angle -240$	280.00	0.00	0.00	Circular
3 $\Phi$ -UV	20% in all phases	248.89 $\angle 0$	248.89 $\angle -120$	248.89 $\angle -240$	248.89	0.00	0.00	Circular
1 $\Phi$ -Ang	10° in phase B	311.12 $\angle 0$	311.12 $\angle -110$	311.12 $\angle -240$	309.54	14.80	4.78	Elliptic
1 $\Phi$ -Ang	20° in phase B	311.12 $\angle 0$	311.12 $\angle -100$	311.12 $\angle -240$	304.86	27.59	9.05	Elliptic
1 $\Phi$ -Ang	20° in phase C	311.12 $\angle 0$	311.12 $\angle -100$	311.12 $\angle -240$	304.86	33.84	11.10	Elliptic
2 $\Phi$ -Ang	20° in phases B and C	311.12 $\angle 0$	311.12 $\angle -100$	311.12 $\angle -220$	298.60	6.25	2.09	Elliptic

### 3.1. Results and discussions

#### 3.1.1. The stator currents data pattern

##### 3.1.1.1. Balanced condition

Figure 9 presents the corresponding Park's vector representation without any fault. In this situation the pattern is a circle centered at the origin of the coordinates. This result is considered as a base line with respect to the case of abnormal condition.

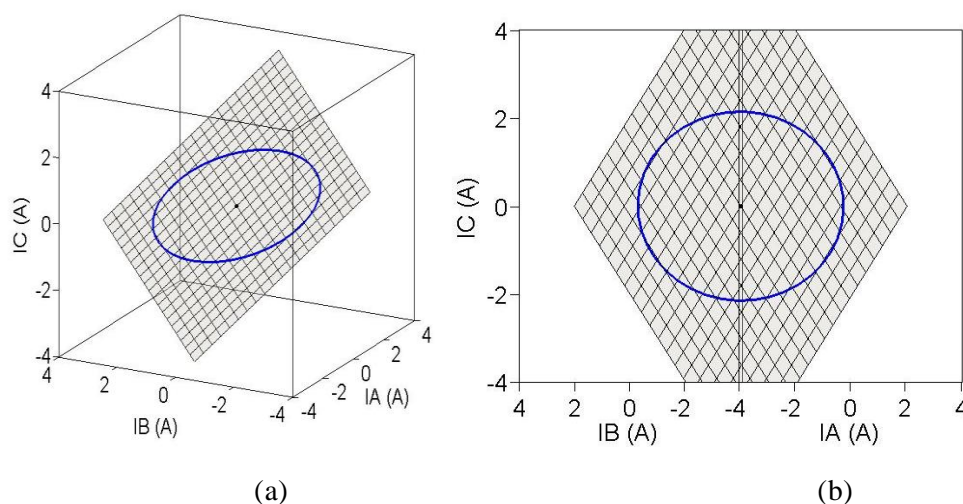


Figure.9. Stator currents pattern for ideal operating condition, (a) 3D view; (b) Orthogonal view

##### 3.1.1.2. Unbalances in the Voltages Magnitude

- Under voltage in phase A and healthy state for phase B and phase C

Figure 10 presents the corresponding Park's vector and 3D stator currents representations with 10% and 20% under voltage-phase A. These figures contain also the plot in the normal operating condition in order to compare it with the faulty condition. It is observed that the elliptic plot corresponding to the unbalanced phase, is clearly deviated from the normal condition circular pattern. The major axis of the ellipse is found to be collinear with the faulty phase (phase A). The severity index of the unbalance is also clear.

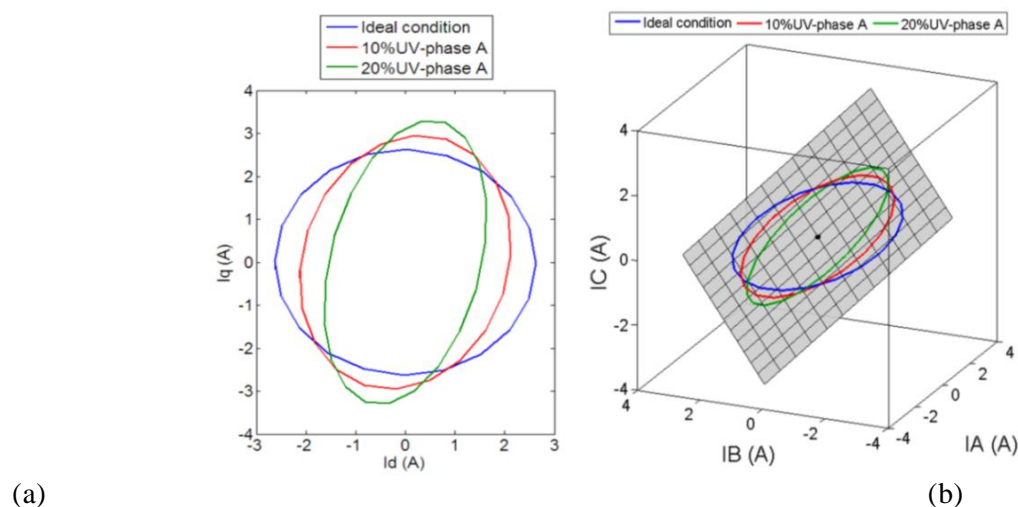


Figure.10 : (a) Current Park's vector patterns; (b) 3D stator current patterns for: 10% and 20% under voltage in phase A

- Under voltage in phase A, B and C

Figure 11 presents the corresponding Park's vector and 3D stator currents representations with 20% under voltage in phase A, B and C. It is observed that the major axis of the elliptic plots, is corresponding to the unbalanced phase, as it was pointed out earlier, this ellipticity is due to the negative sequence component generated by the fault.

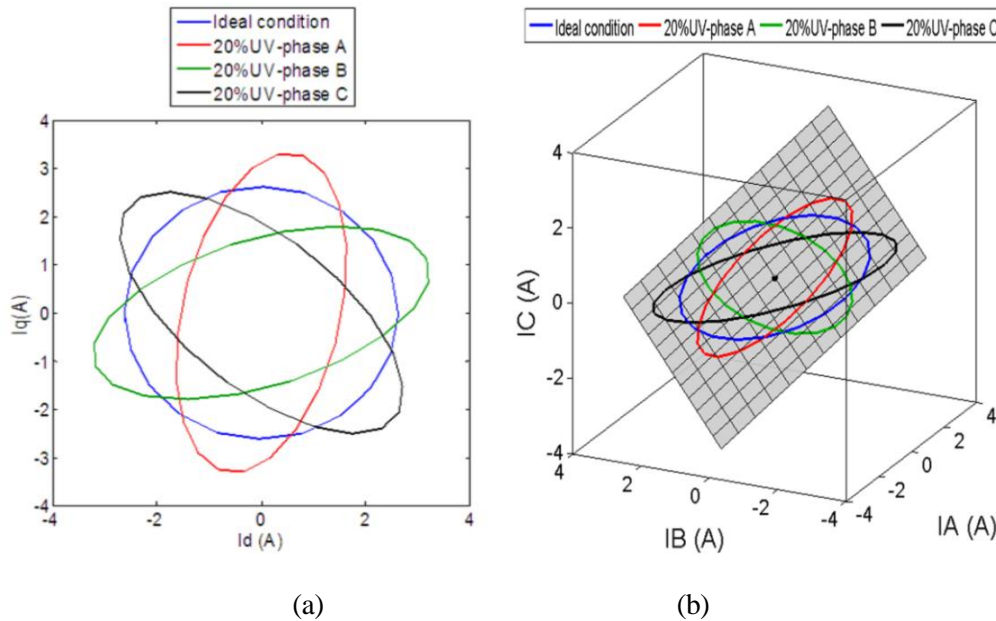


Figure 11. (a) Current Park's vector patterns; (b) 3D stator current patterns for: 20% under voltage in phase A, B and C[6]

- Equal percentage of under voltage in the three phases

The Park's vector pattern in case of an equal percentage of under-voltage in the three phases A, B, and C is illustrated by Figure 12; the plots are in circular forms, the radius is inversely proportional to the increase in the percentage of the unbalance, and also lead to the decrease of the torque. It should be noted that these signs, were considered in [21] as equal percentage degradation in all phases of stator winding fault.

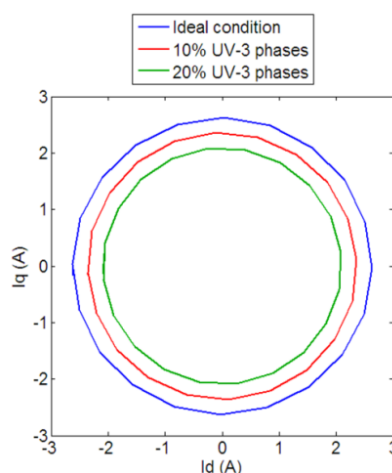


Figure. 12. Current Park's vector pattern for 10 and 20% under voltages in all phases

### 3.1.1.3. Unbalance in the voltage phase

- For ( $10^\circ$ ) and ( $20^\circ$ ) displacement angle of phase B

To refer the most dangerous imbalance is the unbalanced in the voltage phase, because the increase of

the negative sequences is more significant. Table 1, illustrates the imbalance in the voltage phase angle which is  $10^\circ$  and  $20^\circ$  (small values) to show the dramatic impact of this kind of imbalance on the motor performance. Fig.13 presents the stator currents plots with  $10^\circ$  and  $20^\circ$  angle displacement of phase B.

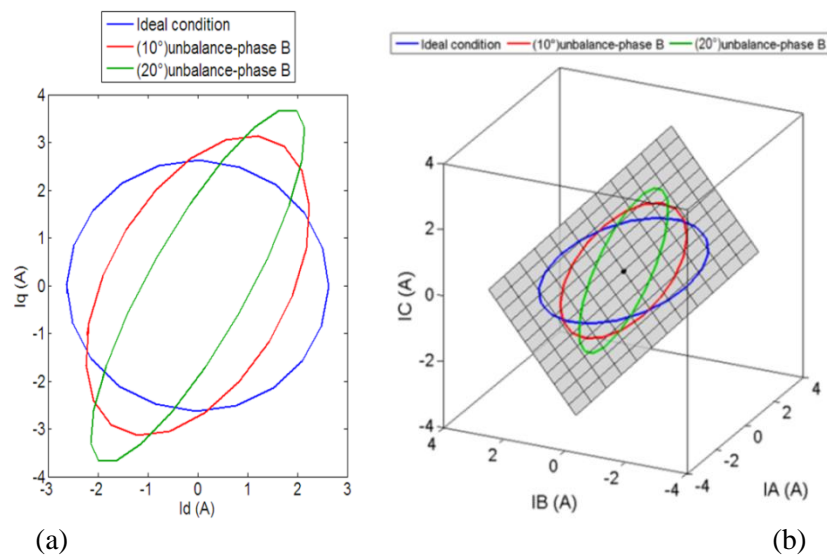


Fig.13: (a) Current Park's vector patterns; (b) 3D stator current patterns for: ( $10^\circ$ ) and ( $20^\circ$ ) angle displacement in phase B [6]

- ( $20^\circ$ ) Displacement of Angle's Phase (B), (C) and (B, C):

Fig.14 presents the corresponding Park's vector and 3D stator currents representations with  $20^\circ$  displacement angle of Phase B, C and B,C.

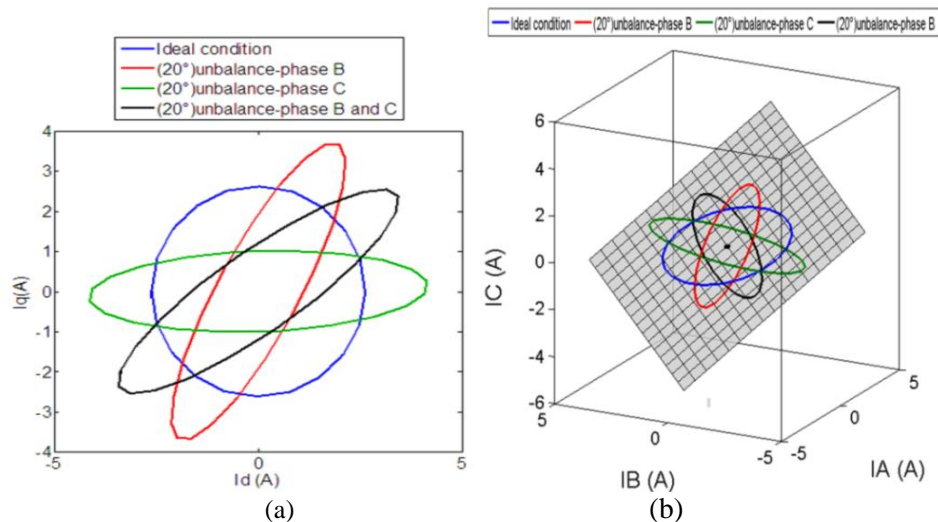


Figure.14. (a) Current Park's vector patterns; (b) 3D stator current patterns for  $20^\circ$  angle displacement in phase (B), phase (C)

### 3.1.2. The enhanced Park's vector approach

#### 3.1.2.1. Balanced condition

Figure15 presents the Park's vector modulus and its spectrum in normal circumstance. It was theoretically predicted that in this condition, the EPVA signature would be free from any spectral component.

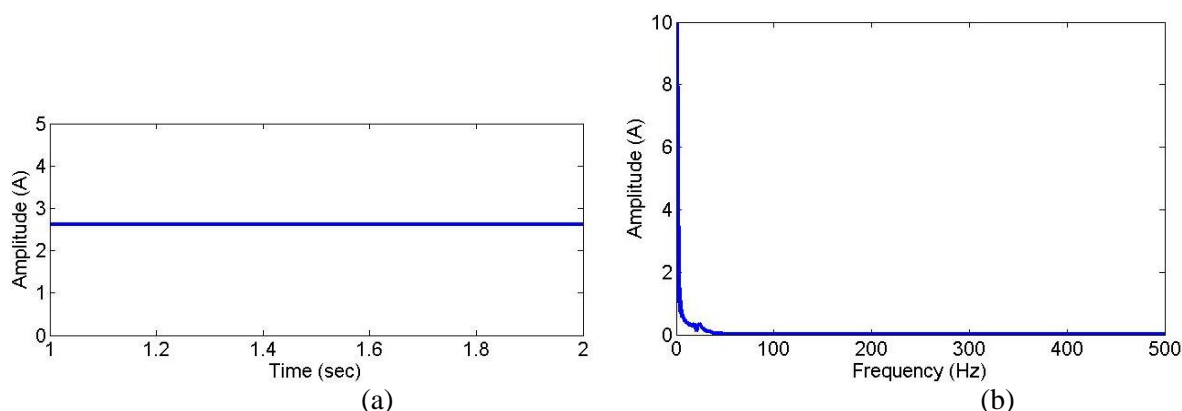


Figure.15. (a) The motor current Park's vector modulus; (b) spectrum of the vector Park modulus in normal operation condition

### 3.1.2.2. Unbalances in the voltages magnitude

Figure 16 presents the Park's vector modulus and its spectrum with 10% and 20% under voltage in phase A. It can be seen that the amplitudes of the  $2fs$  (100Hz), are clearly appeared compared to the normal case (0.4 A for 10% unbalance and 0.8 A for 20% under voltage).

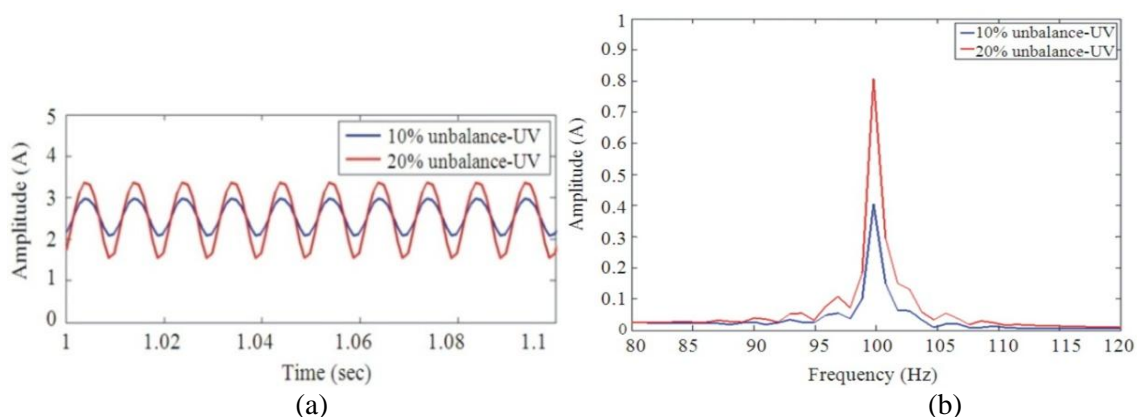


Figure.16. (a) The motor current Park's vector modulus; (b) spectrum of the vector Park modulus around the (100 Hz) in case of 10% and 20% under voltage

### 3.1.2.3. Unbalances in the voltages phase

Figure 17 presents the Park's vector modulus and its spectrum with  $10^\circ$  and  $20^\circ$  displacement angle of Phase B. It can be seen that the amplitude of the  $2fs$  (100Hz) is increased compared to the under voltage cases (0.7A for  $10^\circ$  and 1.3 A for  $20^\circ$ ), which explain the severity of this kind of unbalance.

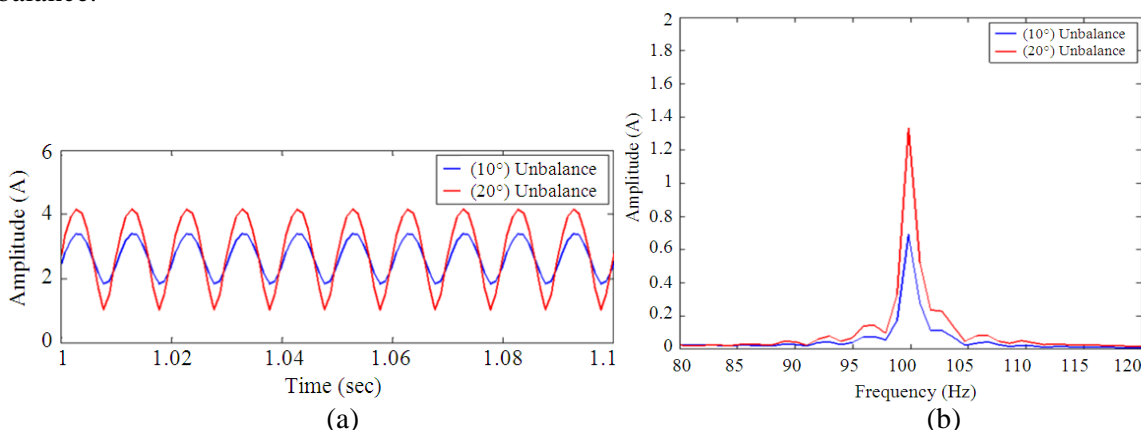
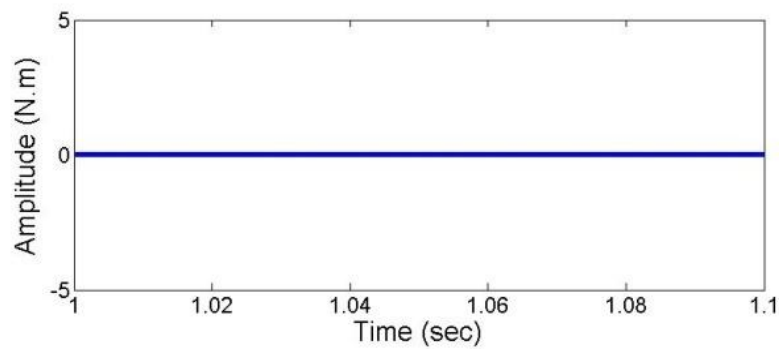


Figure. 17. (a) The motor current Park's vector modulus; (b) spectrum of the vector Park modulus around the (100 Hz) in case of  $10^\circ$  and  $20^\circ$  angle displacement

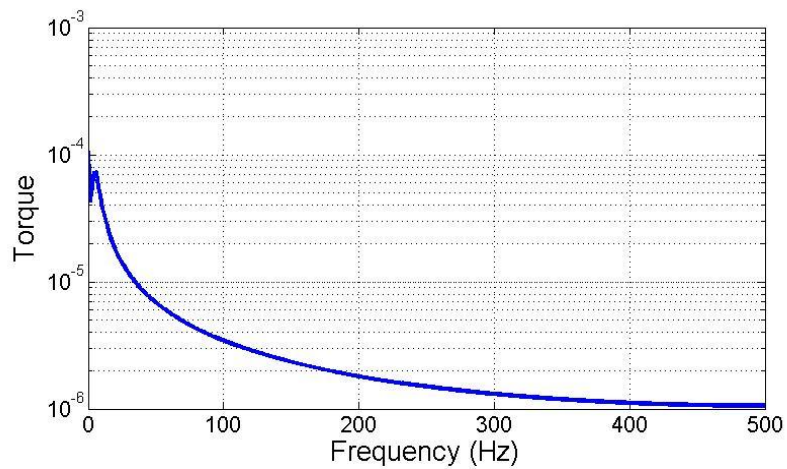
The final stage in the investigation is devoted to distinguishing the anomaly, by using the THA technique, and that is the content of the next section. 3.1.3. Torque Harmonic Analysis (THA).

### 3.1.3.1. Balanced conditions

Figure18 presents the temporel signal of the torque and its spectrum in normal operation condition. The THA signature would be clear from any spectral component.



(a)



(b)

Figure.18. (a) Temporal signal of the Torque; (b) torque spectrum in normal operation conditions



### 3.1.3.2. Unbalances in the voltages magnitude

Figure 19 presents the temporal signal of the torque and its spectrum with 10% and 20% under voltage in phase A. It can be seen that the amplitudes of the  $2fs$  (100Hz), are clearly appeared.

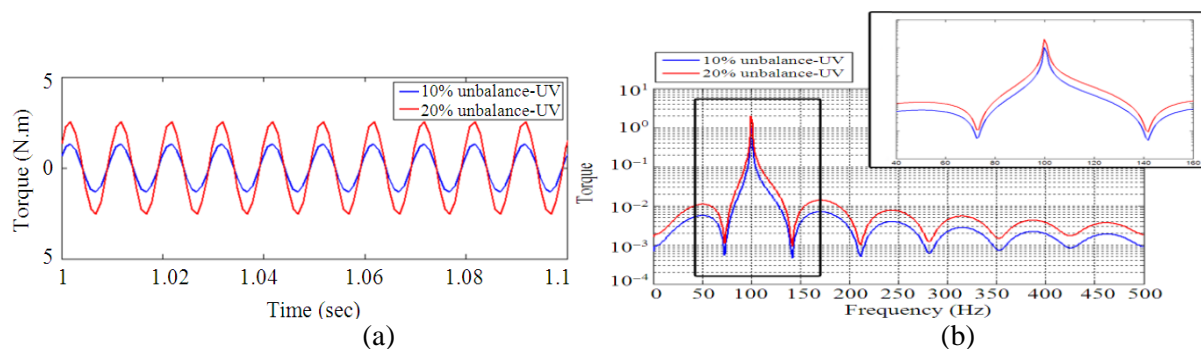


Figure.19. (a) Temporal signal of the Torque; (b) torque spec-trum in case of 10% and 20% under voltage

### 3.1.3.3. Unbalances in the Voltages Phase

Figure 20 presents the temporal signal of the torque and its spectrum with  $10^\circ$  and  $20^\circ$  displacement angle of Phase B. The amplitudes of the  $2fs$  (100Hz), are clearly appeared.

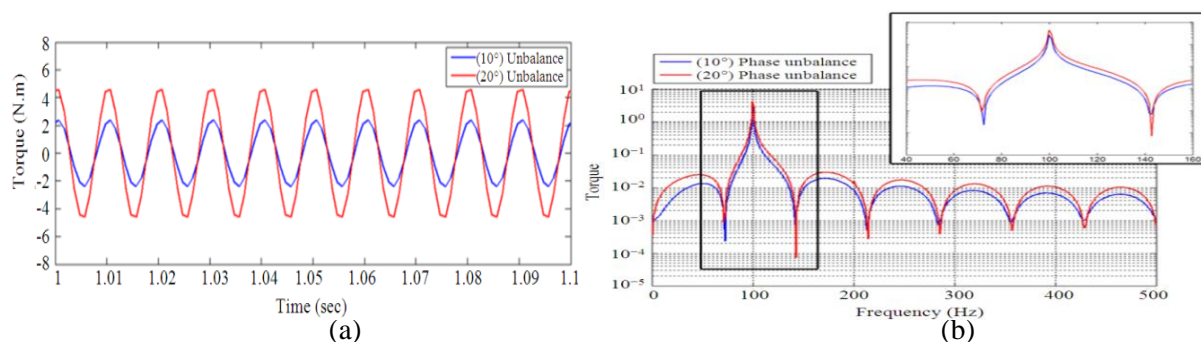


Figure. 20. (a) Temporal signal of the Torque; (b) torque spectrum in case of  $10^\circ$  and  $20^\circ$  under voltage

## 4. CONCLUSION AND PERSPECTIVES

This paper has described the different effects of the imbalanced voltages on the performance of induction motors and the similarity of the signatures of voltage unbalance and stator winding fault. This study is based on numerical simulation has showed this clear similarity. The obtained elliptic patterns and the  $2fs$  harmonic responses generated in the spectrum of the Park's vector modulus are not sufficient for precis diagnosis, because these fault signatures in other works are frequently considered as correct indicators of a stator winding fault. Therefore, these techniques in such situations show faults generally (stator asymmetry). Hence, according to the proposed algorithm, the significant influence on the 2nd harmonic of the torque spectrum (THA), has helped to conclude that this technique provide an assuring indication about voltage unbalance and its severity.

In the same context, we can consider the following perspectives:

- Realizing the experimental tests and compare the results with those obtained by simulation based on mathematical model
- Diagnosing the machine in presence of combined faults (electrical and mechanical)
- Using advanced diagnosis tools (fuzzy logic, neural network...)

**APPENDIX**

The induction motor parameters

Stator resistance	10 $\Omega$
Rotor resistance	6.3 $\Omega$
Stator inductance	0.4612H
Inductor rotor	0.4642 H
Mutual Inductance	0.4212 H
Motor moment of inertia	0.02 Kg. M <sup>2</sup>
Viscous friction coefficient	0.00N.m / Rd / s
Number of pole pairs	2
Rated Speed	157 rad / sec
Rated power	0.75 KW
Supply voltage and current peaks values for each phase	311.12 (V), 2.14 (A)

**ACKNOWLEDGMENT**

The authors acknowledge the contributions of Unit of Renewable Energies in the Saharan for the support and cooperation. Also the authors would like to thank the Department of Electromechanical Engineering- Annaba university members for their valuable help.

**REFERENCES**

- [1] Bouras S., Guedri A., 2006. Analyse et synthese des defaillances simultanees au stator et au rotor des moteurs asynchrones. Revue des sciences et de la technique « Synthèse »,15 : 107-113.
- [2] Benamira N., Neciabia A., Bouraiou A., 2016. Detection du desequilibre de tension d'alimentation en vue de diagnostic de la machine asynchrone , African review of science, technology and developpement, 01 (01) :49-58.
- [3] Cakır, A., Çalış H., Küçükşille E.U., 2009. Data mining approach for supply unbalance detection in induction motor. Expert systems with applications, 36: 11808-11813.
- [4] Quisque, E.C., Lopez-Fernandez X.M., Mendes A.M.S, Marques C.A.J., Palacios J.A., 2011. Experimental study of the effect of positive sequence voltage on the derating of induction motors under voltage unbalance. Proceedings of the IEEE International Electric Machines and Drives Conference, May 15-18, IEEE Xplore Press, Niagara Falls, 908-912.
- [5] Paragsan P., Manyage M., 2006. Loss of life in induction machines operating with unbalanced supplies. IEEE Trans. Energy Conversion, 21: 813-822.
- [6] Benamira N., Faouzi R.M., Bouraiou A., 2013. The investigation of induction motors under abnormal condition. Online journal of science and technology. 3(4), 150-158.
- [7] Donolo P., Bossio G., Angelo C.D., 2011. Analysis of voltage unbalance effects on induction motors with open and closed slots. Energy Conversion & Management, 52: 2024-2030.
- [8] Cruz S.M.A., Cardoso M.A.J., 2001. Stator winding fault diagnosis in three-phase synchronous and asynchronous motors by the extended parks vector approach. IEEE Transaction on Industrial application. Applic, 37: 1227-1233.
- [9] Martins J.F., Pires V.F., Amaral T., 2011. Induction motor fault detection and diagnosis using a current state space pattern recognition. Pattern Recognition Letters, 32: 321-328.
- [10] Pires, V.F., J.F. Martins and A.J. Pires, 2010. Eigenvector/eigenvalue analysis of a 3d current referential fault detection and diagnosis of an induction motor. Energy Conversion & Management, 51: 901- 907.
- [11] Samsi R., Ray A., Mayer J., 2009. Early detection of stator voltage imbalance in three-phase induction motors, Electric Power Systems Research, 79: 239–245.



- [12] Nejari H., Benbouzid M.E.H., 2000. Monitoring and diagnosis of induction motors electrical faults using a current park's vector pattern learning approach. Proceedings of the International Conference Electric Machines and Drives, May 9-12, IEEE Xplore Press, Seattle, WA, : 275-277.
- [13] Gnacinski P., 2008. Effect of unbalanced voltage on windings temperature, operational life and load carrying capacity of induction machine, *Energy conversion & management*, 49: 761–770.
- [14] Ching-Yin L., Bin-Kwie C., Wei-Jen L., Yen-Feng H., 1998. Effects of various unbalanced voltages on the operation performance of an induction motor under the same voltage unbalance factor condition. Proceedings of the Industrial and Commercial Power Systems Technical Conference, May 11-16, IEEE Xplore Press, Philadelphia, PA, 51-59.
- [15] Rohan S., Ray A., Mayer J., 2009. Early detection of stator voltage imbalance in three-phase induction motors. *Electrical Power Systems Research*, 79: 239-245.
- [16] Bouras A. & al., 2014. Investigation on the diagnosis of simple and combines mechanical faults in asynchronous motor based electric drives. *American Journal of Applied Sciences*, 11 (6): 994-1004.
- [17] Zarei J., Poshtan Javad, 2009. An advanced Park's vector approach for bearing fault detection, *Tribology International*, 42 :213–219.
- [18] Benbouzid M.E.H., Vieira M., Theys C., 1999. Induction motors' faults detection and localization using stator current advanced signal processing techniques. *IEEE Transaction on Power Electrical*, 14: 14-22.
- [19] Mirabbasi D., Seifossadat G., Heidari M., 2009. Effect of unbalanced voltage on operation of induction motors and its detection. Proceedings of the IEEE International Conference of Electrical and Electronics Engineering, IEEE Xplore Press, Bursa, 189-192.
- [20] Khoobroo M., Krishnamurthy M., Fahimi B., Wei-Jen L., 2008. Effects of system harmonics and unbalanced voltages on electromagnetic performance of induction motors. Proceedings of the 34th Annual Conference of IEEE Industrial Electronics, Nov. 10-13, IEEE Xplore Press, Orlando: 1173-178.
- [21] Modak A.J., Inamdar H.P., 2010. Computer-aided simulation model of stator groundwall insulation of induction motor based on current park's vector approach. *International Journal of Computer Applications*, 9: 24-33.